eTraverse
GEOGRAPHICAL INSTITUTE
The Indian Journal of Spatial Science

Vol. II No. 1 — 2011

Article 2

Topographic Analysis of the Dulung R. Basin

Prof Ashis Sarkar
Priyank Pravin Patel

GEOGRAPHICAL INSTITUTE
1949–50

eTraverse
GEOGRAPHICAL INSTITUTE
The Indian Journal of Spatial Science

Vol. II No. 1 — 2011

Article 2
Topographic Analysis
of the Dulung R. Basin

Prof Ashis Sarkar
Priyank Pravin Patel

Paper accepted on 01.10.2010

Published by
Prof Ashis Sarkar

on behalf of
The Geographical Institute
Department of Geography
Presidency College
86/1 College Street, Kolkata 700073, India
geographicalinstitutepc@gmail.com
Ph. +91 33 2241 1960 Ext. 206

Typeset and layout by
Computer Club
ccprepress@gmail.com

Topographic Analysis of the Dulung R. Basin

Prof Ashis Sarkar
Priyank Pravin Patel

A drainage basin is the most fundamental unit of geomorphological study and topography constitutes the first essential component of its geosystem / ecosystem. It forms the base upon which lie the geodata layers of all the elements of geography, viz., soil, surface water, vegetation, settlement pattern, landuse pattern, transport network, and all possible social and economic expressions of human behaviour. While addressing the issues of regional development, thematic maps are often prepared using attribute databases as graphic overlays on a reference map generated by geodetic control network (GCN) and topographic / elevation database (tBase) - hence the importance of topographic analysis in geography. It helps to perceive the spatial association between tBase and human elements and thereby facilitates us to understand the world around us better by enabling us to develop spatial intelligence for logical decision making in order to formulate strategies for development of a region.

Introduction

A contour profile is simply an outline produced by the plane of a section as intersecting the ground surface. It is obtained by interpolation of contour elevations on a chosen scale and along a chosen line on a map transverse to the grain of the region. Naturally, it depicts the ground form in a more comprehensible and precise format. A series of profiles at regular intervals of space and time are usually drawn to understand the changes in topographic pattern of a landscape. When these profiles are arranged and drawn on a single frame, a superimposed profile is produced. This helps to identify breaks in slope, and accordant summit levels / planation surfaces. The highest parts of the superimposed profiles, as viewed in the horizontal planes of the summit levels from an infinite distance produces the composite profile. It represents the skyline with a defined perspective. To extract the panoramic effect of the landscape projected, profiles are framed by sequentially drawing the profiles, one after the other, starting from the foreground to the distant part and successively erasing the part obscured by the former profiles. Profile analysis of the Dulung basin has been done to comprehend the topographic properties of the basin terrain.

Methodology

- Drawing of profile lines across the basin surface at 1 km interval distance (Fig.1) across the basin surface generated from ASTER GDEM tiles with the help of hydrological software and extraction of transverse cross-sections to create serial of selected profiles and superimposed profiles in order to ascertain different probable accordant summit levels or planation surfaces.
- Computation of profile statistics of above cross-sections to show variations in surface form.
- Overlaying of digitized contours across the basin surface and conversion of the contour lines to contour polygons and enumerating the area of each elevational slab thus derived
- Clipping of contour polygon zones falling within each examined constituent sub-basin of the Dulung and enumerating the area of each elevational slab thus derived
- Basin hypsometric analysis of the Dulung Basin and its major sub-basins is performed after Strahler (1952). Estimation of the hypsometric integral (H.I.) for lower order basins (1st to 3rd Strahler orders) is done using Pike & Wilson's (1971) modification of the Strahler method where,

  H.I. = (Mean Basin Elevation – Minimum Basin Elevation) / Basin Relief)

  This method is useful especially for the small lower order basins, since in areas of low relief where these are often situated, sufficient number of contour lines often do not traverse across the basin area, to enable derivation of satisfactory elevational slabs.

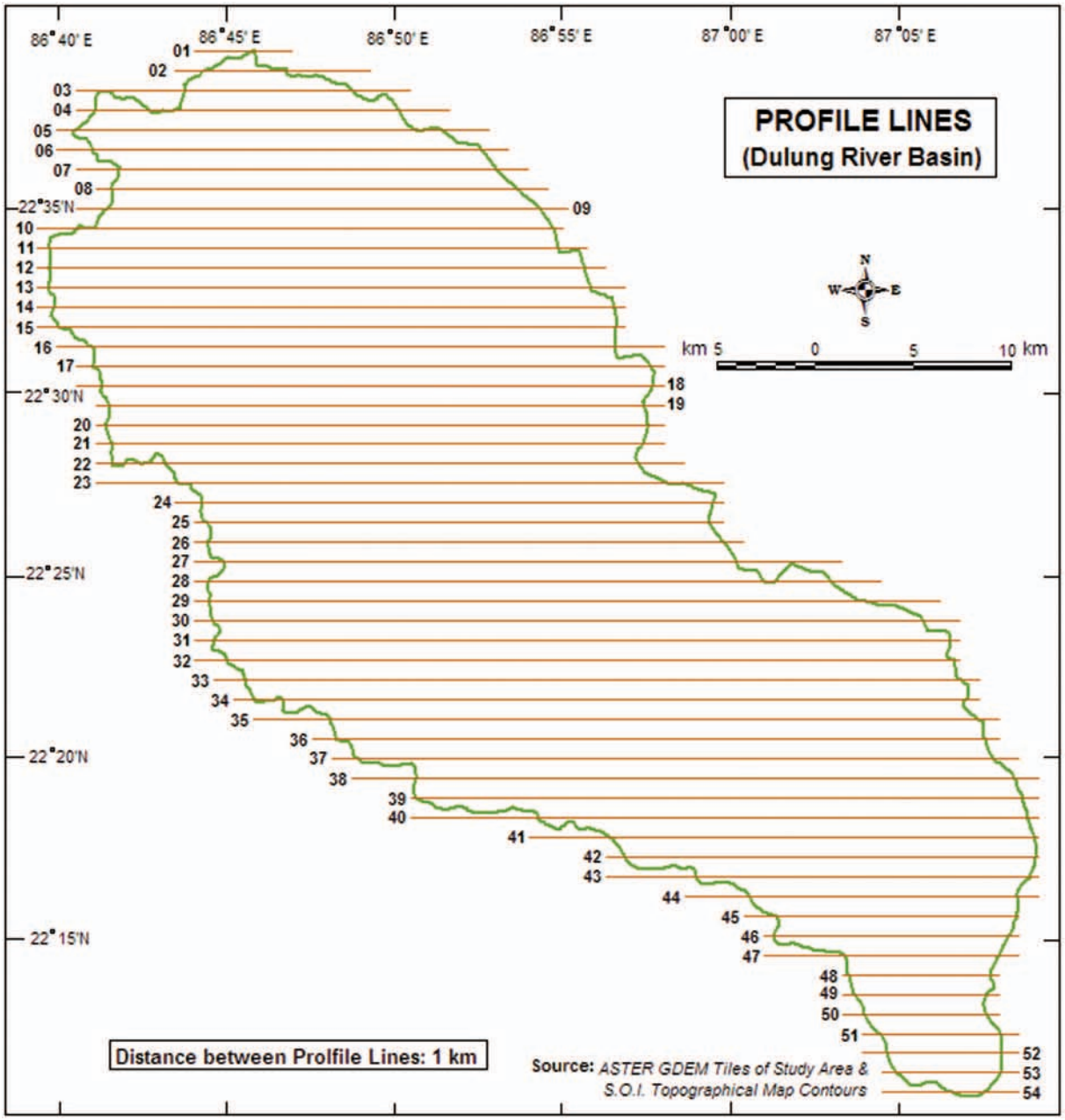

Fig. 1: Profile Lines

- Drawing *hypsometric curves* for the higher 6th to 4th Strahler order basins by plotting (a / A) against the (h / H) values and algebraically computing the *hypsometric integrals* more accurately for each basin
- Performing statistical fitting of the hypsometric curves using curve-fit software.
- Performing a *multivariate analysis* between hypsometric integral, network parameters, shape parameters and morphometric parameters using SPSS for the Dulung River and its major sub-basins (why not just given this line instead of the 3 sub-points above)

Topographic Sections

In all 54 surface profiles have been taken across the Dulung river basin using a combination of DEM, contour and spot elevation data. The most significant of these profiles have been stacked together in a serial of profiles keeping intact the perspective of view to show the elevation changes over the area (Fig. 2). Profiles P05 and P11 taken across the upper basin crystalline complex shows the drastic increase in height to the west in the northern part of the basin. The surface grades down in a series of hills to the gentler plain in the east – giving an indication of there being more than

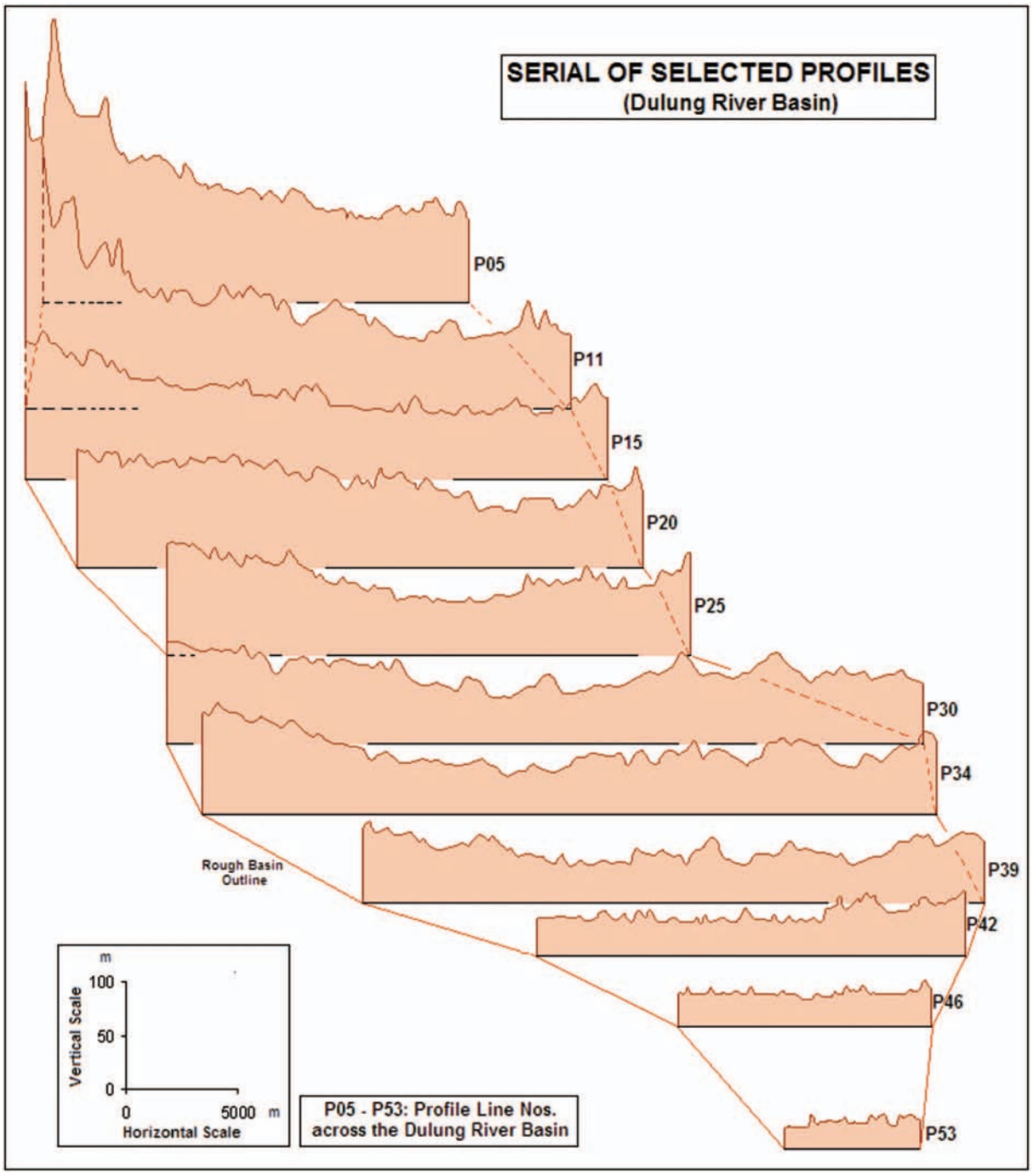

Fig. 2: Serial Profiles

one accordant summit level and probable planation surface in this cross-section. Profile P15 cuts across the transition zone between the northern complex and the gentle, open valleys to the south. The western half of the profile is still significantly more upstanding than its eastern counterpart but the difference is much lesser than before. To the east the present narrow plain of the Dulung is spied. Profiles P20, P25, P30 and P34 traverse across the central Dulung Basin. Sections of the western ridges are prominent while portions of the lower eastern ridges and residual hills show up in these profiles.

The most significant feature is the development of the broad central valley floor over which the Dulung meanders in this stretch. Profiles P39 and P42 are taken across the lower stretch of the Dulung's course. The valley floor is much broader here and constitutes much of the profile. The western ridges have almost died out and the topography to the east is now relatively more upstanding, formed often

of lateritic caps, and comprises of the dissected minor water divide that separates the valleys of the Champa Nala and the Koali Khal which are the last tributaries that the Dulung receives before its confluence. The last two profiles P46 and P53 are taken near the Dulung's mouth. The basin has narrowed considerably while the Dulung's valley floor has broadened and now constitutes the entire profile. It is quite an extensive floodplain with the few very minor upstanding portions often being a result of much localized deposition by the river itself that has built up extensive sandbars along this stretch. The narrowing of the profile lines is also indicative of the severe flooding the lower portion of the Dulung is subjected to since all the waters gathered so far upstream are now channelised into this constricted, low floodplain. Thus when the river is in spate here, its waters often spreads out over the entire profile portion.

The superimposition of all 54 extracted profiles rendering the resultant graph too cluttered for a proper examination, average elevation values have been derived grouping every three profile lines together. The resultant graph (Fig. 3) reiterates the conclusions drawn form the above analysis of serial profiles. The eastern side of the basin barely rises above 100 m while the western portion consists of all the higher hills and ridges. The superimposition also reveals quite clearly the probable accordant summit levels or planation surfaces within the basin area. Four such surfaces or levels can be broadly identified:

1. Between 20 — 40m stretching right across the lower basin is the lowest surface that consists of the Dulung's broad floodplain.
2. Between 60 — 80m in the eastern portion of the basin lies the accordant summit level of the lower eastern ridges that are laterite capped and their piedmont zone. They grade down to the gentle floodplain towards the west.
3. Between 90 — 130m in the western portion of the basin lies the accordant summit level of the relatively higher western ridges and their piedmont zone. They grade down to the gentle floodplain towards the central basin area basin slightly grading upwards to the east.
4. Between 170 — 200m in the western basin fringe lies the accordant summit level of the hills situated in the northern complex and the eastern Chotonagpur fringe plateau surface.

The superimposed profile lines further demonstrate how the land grades between the

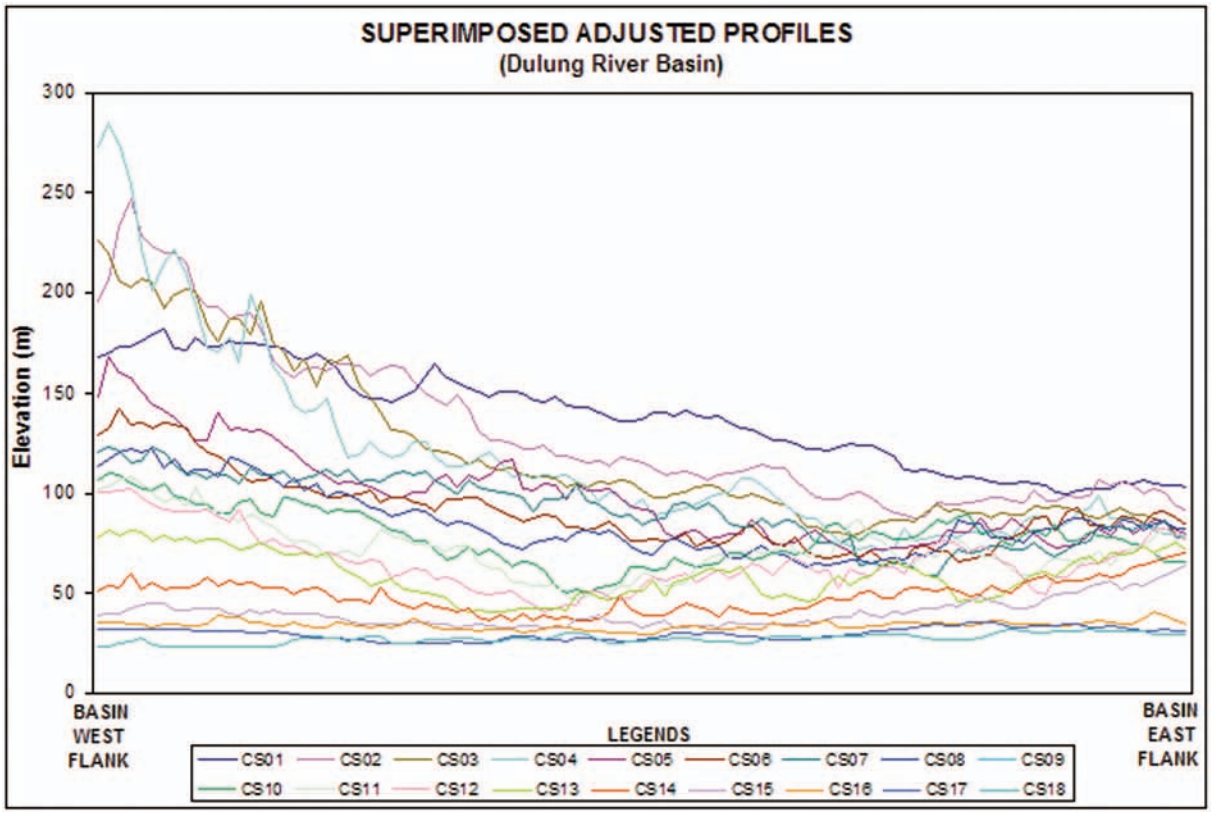

Fig. 3: Superimposed Profiles

various topographic levels, revealing a stark difference in altitude between the two planation surfaces in the eastern and western section of the area while the central planation surface – the Dulung's floodplain lies betwixt the former two, to which they both grade down. The greater ruggedness of the western section is emphasised. Profile-line statistics have been enumerated to mathematically deduce the nature of relief along the extracted profiles by computing the mean elevation, range, standard deviation and grid-to grid altitudinal difference of the elevation pixels that lie along each profile-line (Fig. 4). They bear out the following facts—

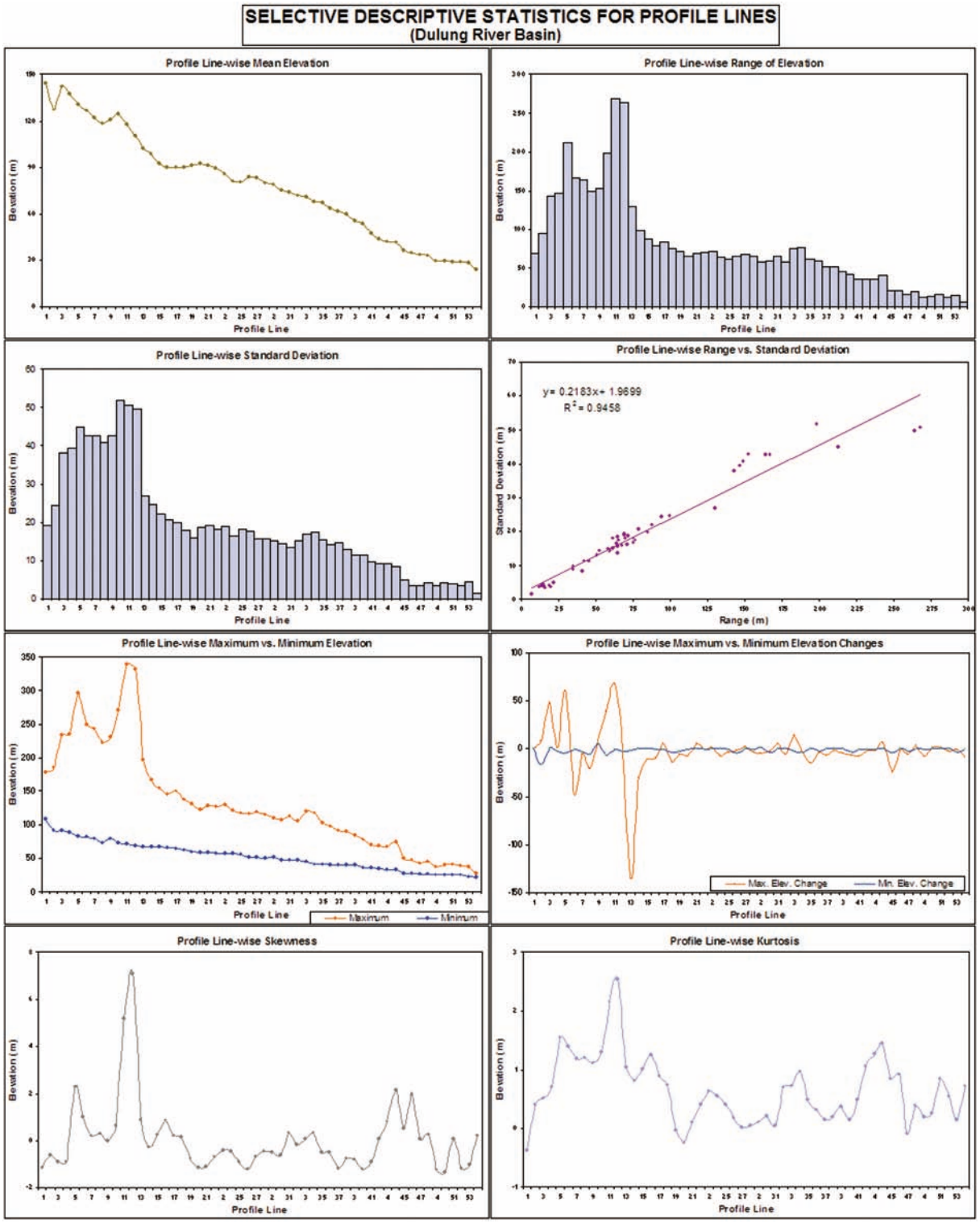

Fig. 4: Profile Parameters

1. The mean elevation in the northern part of the basin is relatively more than that in the southern part. The mean elevation also decreases sharply form the northern part (P01 to P15) from about 150m to 90m and then steadies out around 70m till P27. It then decreases at a constant rate till P41 (50m) before leveling out again for the remainder.
2. Mean elevation of the sequentially drawn profiles decreases continuously and gradually from the source areas towards mouth (P01 – P02, P03 – P08, P10 – P16, P19 – P25, and P26 – P54).
3. The profile-wise elevation range shows three distinct trends. Its above 150m for most of the northern profiles (P01 to P13), then holds steady around 70m for the central basin area (P14 to P35) and then decreases markedly to below 30m for the last few profiles (P40 to P54).
4. Range of elevation gradually decreases towards mouth with modes at P05, P11, P34, and P44. The distribution is typically positively skewed with tail towards right.
5. The standard deviation values per profile line too follow the above trend with the highest values being recorded for the northern profiles that traverse over both the western high hills and the eastern lower plains resulting in a greater range of elevation values. The least deviation values are seen over the lower basin where the topography is almost uniform with almost no sharp changes in relief. The profile-line-wise elevation range and standard deviation correlate strongly (R^2 = 0.95) bearing out the above relationship.
6. Distribution of variance is also multimodal with modes at P05, P10 and P34. However, on the whole, it produces a positively skewed distribution.
7. That the range of elevation values decreases markedly towards the southern profiles is also seen when profile-line-wise maximum and minimum values are plotted against each other. There is a gentle but steady decrease in the minimum values. The maximum values fluctuate above 200m where the lines pass over high hills and plateau fringes in the northern portion but then decline steadily and are almost similar to the minimum values in the lower basin area.
8. Standard deviation values increase with increasing range of elevation, the two being related by the equation: $\sigma = 0.2583\ R + 1.9699$ (R^2 = 0.95).
9. Profile line-wise elevation changes have been computed by comparing the change in maximum and minimum elevations across consecutive profiles. An almost straight line of the minimum elevation changes shows that it has declined at a uniform rate, as stated before.
10. The maximum elevation changes fluctuate in the northern part of the basin – the line rises sharply as profile lines pass over hills and then dip sharply as the next line passes over the adjacent valleys. However this line too steadies out over the middle and lower basin areas, showing that the rate of maximum elevation decrease in therein is uniform.
11. Computed skewness and kurtosis values for each profile too show three distinct groupings. Skewness values are markedly positive in for the northern complex profiles, negative for the middle basin area and fluctuate between positive and negative values for the remainder. The highest kurtosis values are recorded for the northern profiles and the lowest for profiles of the middle basin.

Thus, it is seen that the changes in relief marries closely with the hypsometric analysis of the major sub-basins. The variation of relief is apparent in the extracted cross-sections and the difference in elevations along them clearly shows up the different landscapes constituting the basin, being heavily dependent of the geology. This in turn influences basin relief and consequently impacts on the hypsometric integral derived.

Hypsometric Analysis

A hypsometric curve is an empirical cumulative distribution function of elevations in a catchment area. It may also be viewed as a continuous function and graphically displayed as an x–y plot with elevation on the ordinate and area above the corresponding elevation on the abscissa. Such curves are usually drawn in non-dimensional standardized form by scaling elevation and area by the maximum values so that the similarity of watersheds can be explored. Hypsometric curves may take different forms, the geometry of which describes the state of a landscape defined by the magnitude of the hypsometric integral. The shape of the curve, the

hypsometric integral and the regression parameters of the best-fit statistical curves can be conveniently used as descriptive parameters for the purpose of comparison and classification. The variation of the hypsometric integrals can be associated with the network parameters, shape parameters and morphometric parameters of drainage basins.

Historically, hypsometry has been used as an indicator of the geomorphic form of the catchments and landforms. It is strongly dependent on the channel network and catchment geometry. Computationally, it refers to finding the distribution of elevations as a function of area occupied by each contour interval within a terrain unit, e.g., a topographic map sheet. The idea of hypsometry was introduced by Langbein & Basil in 1947 and was later extended by Strahler (1952) to include the percentage hypsometric curve (area-altitude curve) and the hypsometric integral. Using the dimensionless parameters, curves can be described and compared irrespective of the true absolute scale. Curves show distinctive differences both in sinuosity of form and in proportionate area below the curve, termed as the hypsometric integral (HI).

The prime hypsometric parameter is defined as a volume bounded by the base and summit planes of a given area (A), and the total height (H) from the base to the highest elevation. On a map, beginning from the lowest elevation (base-level) progressively upwards through the increasing values of 'h', i.e., the inter-contour interval, the areas within each contour interval is measured. With each successive increase in height, the area increases by some new value of 'a', i.e., the area bounded by two successive contours. This progression is cumulative and when plotted on a rectangular frame, the relative values of h/H (y) and a/A (x) yield what is called, the hypsometric curve. Thus for y = 0, all heights lie above the datum plane, i.e., x = 1. The area below the hypsometric curve is computed to determine the hypsometric integral that represents the unconsumed volume as a proportion within the basin delimited by the base plane, the summit plane and perimeter.

Various factors influence the shape of the hypsometric curve and its location with respect to the (0,1) – (1,0) diagonal reflects the nature of hypsometric integral. Direct interpretation of a family of hypsometric curves, and their possible interrelationships, is not straightforward but some generalizations can be made. Overall, the HI broadly denotes the degree of upland dissection. The upward – convex curves may typify a relatively high elevation terrain equivalent to what Davis (1899) called a youthful topography. Almost straight-line curves with minimum sinuosity represent progressively more mature topography, while the initially steeply downward sloping and predominantly upward – concave curves are characteristics of the late stage of erosion.

Thus, stages of youth, maturity, and old age in regions of homogeneous rock give a distinctive series of hypsometric forms, though mature and old stages give almost identical curves unless monadnocks are present. Hence, to elucidate more aptly on the physical state of basin development, the above terminology is replaced by an inequilibrium state (youth), an equilibrium state (mature), and a monadnock state (old). However, hypsometric curves and resultant hypsometric integrals cannot be treated as an absolute indicator of basin evolution since various combinations of the operational intensity of the geomorphic agents; geochronology and tectonics can also lead to similar curves in proximate locations. Thus, hypsometric data is not always equivocally interpretable and as a result, deductions require very careful considerations. The major objectives of this chapter are to analyse the observed and statistical best-fit hypsometric curves of the Dulung River along with its 5th and 4th order sub-basins, to derive their hypsometric integrals and to associate the variations in hypsometric integrals with network, morphometric and shape parameters of the basins.

Hypsometric Plots

Hypsometric integrals for the all 3rd order basins were estimated using Pike and Wilson's (1971) approximation method since often these basins were too small to elicit proper values using the Strahler scheme and used in the cluster analysis performed previously and are thus not considered here. The hypsometric curves for each 4th, 5th and 6th order basin have been computed following Strahler (1952) and plotted (Fig. 5). The elevation slabs are commonly uniform in size, except near the basin head or mouth. Thus, the cumulative '*h/H*' values often maintain an arithmetical progression. As a result, deviations from the equilibrium line are caused by the differing values of '*a*' in each elevational slab, which then trigger a cascading effect during computation of the cumulative '*a/A*'

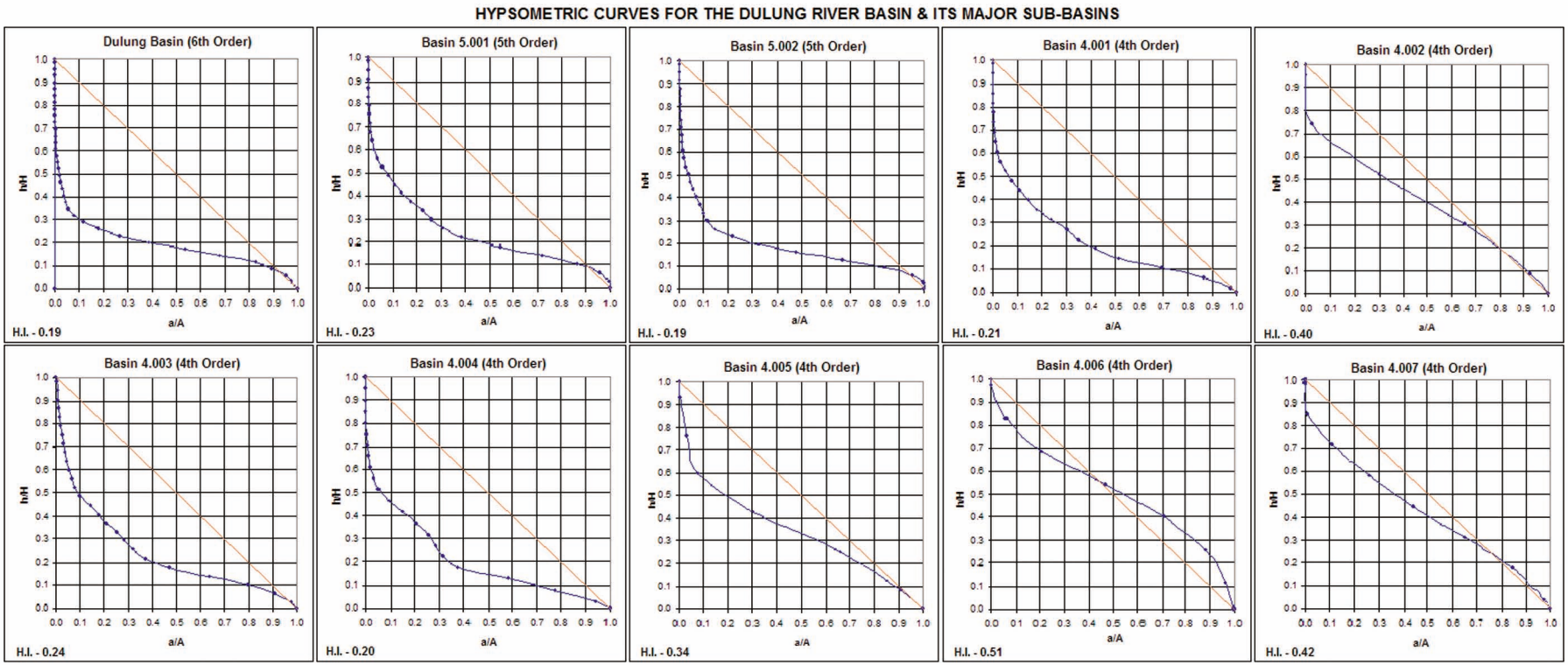

Fig. 5: Hypsometric Plots

values for each basin. When the '*a*' in an elevational slab is approaching minimum values near the basin head and increases little in the subsequent elevation slabs towards the basin mouth, the resultant curve shows an initial steep fall with an increasing distance from the equilibrium line. Marked denudation in the upper reaches and simultaneous / subsequent (or both) accretion in the lower reaches characterize such a basin. Therefore, the elevation slabs in the middle and lower basin reaches, though of the same width elevation-wise are broader as the channel's gradient is much declined, occupying much larger area. With an increase in the values of '*a*', the cumulative '*a/A*' values increase significantly across successive elevation slabs and thus the steeply falling hypsometric curve begins to taper off with a gentle gradient to finally run almost parallel to the abscissa. Such curves represent an old stage of erosion cycle, having steep-sided low hills in the upper catchment region with narrow, entrenched, confined stream defiles, and subsequent valley broadening and floodplain development in the middle and lower reaches.

The greater the disparity of '*a*' values between elevation slabs of the upper and lower reaches, with the smaller values being recorded in the upper catchment, the more elliptic the curve becomes with greater initial downward deviation from the equilibrium line and greater concavity upwards. It is certainly indicative of a marked old stage in the basin's evolution, further attested to by the low hypsometric integrals (below 0.35). A reversal of these conditions produces a curve that is a mirror image of the above and representative of a youthful stage with higher hypsometric integrals (above 0.60). It signifies the presence of most of the basin area in the upper catchment region as a prequel to the eventual sculpting and enlargement of the basin

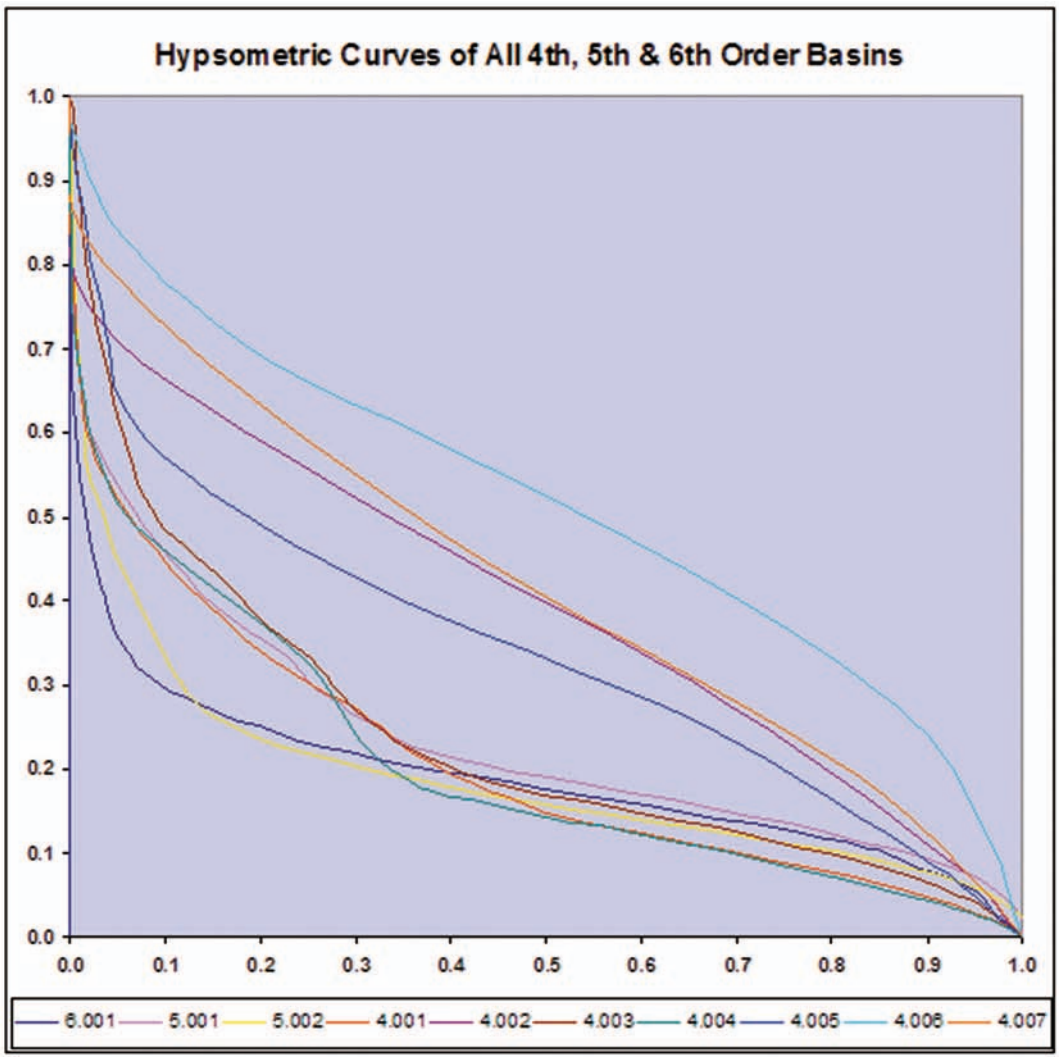

Fig. 6 Hypsometric Plots Superimposed

mouth and lower and middle reaches of the stream with continuous denudation. Thus hypsometric curves of different time periods of a single basin plotted on the same frame give an idea about the total volumetric loss due to sub-aerial denudation. With almost similar values of '*a*' for each elevation slab, comes a steadily increasing array of cumulative *a/A* values, devoid of any sudden breaks or leaps, indicative of an almost equal distribution of area across the basin reaches. As such, an almost linear relation is derived between *h/H* and *a/A* values with minimum deviation from the line of equilibrium. Such a curve indicates the mature stage of erosion with *HI* values ranging between 0.35 and 0.60.

The hypsometric curves obtained for the various basins have been superimposed together (Fig. 6). From their attitudes, similar curves can be grouped into families to signify basins in a similar evolutionary / denudational stage. Furthermore, the hypsometric integral (HI) of each of the basins from 3rd to 6th order (Table – 1) have been considered during the clustering process. Five such 'families' can be identified —

Table – 1: Hypsometric Integral of the Dulung and its 42 Sub-Basins

Basin ID	Hypsometric Integral	Basin ID	Hypsometric Integral
3.001	0.25	3.023	0.35
3.002	0.32	3.024	0.40
3.003	0.28	3.025	0.51
3.004	0.24	3.026	0.56
3.005	0.46	3.027	0.50
3.006	0.59	3.028	0.37
3.007	0.30	3.029	0.49
3.008	0.35	3.030	0.57
3.009	0.18	3.031	0.63
3.010	0.22	3.032	0.57
3.011	0.27	3.033	0.48
3.012	0.26	4.001	0.21
3.013	0.15	4.002	0.40
3.014	0.48	4.003	0.24
3.015	0.28	4.004	0.20
3.016	0.38	4.005	0.34
3.017	0.39	4.006	0.51
3.018	0.48	4.007	0.42
3.019	0.42	5.001	0.23
3.020	0.42	5.002	0.19
3.021	0.48	6.001	0.19
3.022	0.37		

Source: Computed by the authors

1. Late youth stage (0.65 ≥ HI > 0.55): There are five basins in this category, viz., 3.031, 3.006, 3.030, 3.032, and 3.026 in the decreasing order of the magnitude of hypsometric integral.
2. Early mature stage (0.55 ≥ HI > 0.45): There are nine basins at this level, i.e., 4.006 (whose gently declining, concavo-convex curve has formed close to the equilibrium line intersecting it along its course) and 3.025, 3.027, 3.029, 3.033, 3.014, 3.018, 3.021, and 3.005 in the decreasing order of the magnitude of hypsometric integral.
3. Late mature stage (0.45 ≥ HI > 0.35): Altogether nine basins are there in this stage, viz., 4.007 and 4.002 (whose curves are almost identical - gently declining, concave upwards, just intersect the equilibrium line in the lower reach) along with 3.020, 3.019, 3.024, 3.017, 3.016, 3.022, and 3.028 in the decreasing order of the magnitude of hypsometric integral.
4. Early old stage (0.35 ≥ HI > 0.25): There are nine basins in this stage, viz., 4.005 (whose curve initially declines sharply but then has a steady rate of decline for the remainder of its course. The curve closer in attitude to that of the 'late mature stage') along with 3.008, 3.023, 3.002, 3.007, 3.015, 3.003, 3.011, and 3.012 in the decreasing order of the magnitude of hypsometric integral.
5. Senile stage (HI ≤ 0.25): There are eleven basins in this stage including the main Dulung basin (6.001), sub - basins of 5.002, 4.004 (whose curve is initially sharply declining before levelling out, concave upwards and has the maximum displacement from the line of equilibrium, forming well below it), 5.001, 4.003, 4.001, 3.001, 3.004, 3.010, 3.009, and 3.013 in the decreasing order of the magnitude of hypsometric integral. The curve for 4.004 is quite interesting — even though the HI suggests the basin to be in the senile stage, a division is seen between the upper part of this basin and the lower half. The curve for the upper part is similar to that for the 'late mature to early old stage' basins while the lower half's curve is similar to that for the 'senile stage' — a classic case of the basin straddling the zone of transition between the dissected upper plateau surface and the gently rolling plains. The curves for basins 5.001, 4.001, 4.003, are more similar to those for the early old stage.

Hypsometric Integral	Basins & Sub-basins
1. > 0.55:	{3.031, 3.006, 3.030, 3.032, 3.026}
2. 0.45 – 0.55:	{4.006, 3.025, 3.027, 3.029, 3.033, 3.014, 3.018, 3.021, 3.005}
3. 0.35 – 0.45:	{4.007, 4.002, 3.020, 3.019, 3.024, 3.017, 3.016, 3.022, 3.028}
4. 0.25 – 0.35:	{4.005, 3.008, 3.023, 3.002, 3.007, 3.015, 3.003, 3.011, 3.012}
5. ≤ 0.25:	{6.001, 5.002, 4.004, 5.001, 4.003, 4.001, 3.001, 3.004, 3.010, 3.009, 3.013}

Best-fit Hypsometric Curves

The x – y plots of the hypsometric frame can be explored for better objectivity in description and analysis. For this a set of models has been selected. These are: linear, quadratic, n^{th} order polynomials, exponential family, power family, yield-density models (Harris), sigmoidal models (MMF), plus a number of user-defined models. For each curve of the seven 4th order, two 5th order and the main 6th order Dulung river basin, all the above have been fitted and their standard error of estimate (S_E) and coefficient of determination (R^2) have been judged with a view to minimizing the S_E and maximizing the R^2. Special software for statistical curve fitting has been used for this and the following five have emerged as the best fit hypsometric curves as follows—

1. Yield-density Model (Harris) : $y = 1 / (a+b^x)$
2. Sigmoidal Model (MMF) : $y = (ab+cx^d)/(b+x^d)$
3. 3rd Order Polynomial : $y = a+bx+cx^2+dx^3$
4. Logistic Model : $y = a /(1+b.e^{-cx})$
5. Rational Function : $y = (a+bx)/(1+cx+dx^2)$

The results (Table – 2) may be analysed in the following manner. Harris model emerged best fit for one of the 4th order, one of the 5th order and the main Dulung basin, logistic model for the remaining 5th order basin only. The remaining basins fit best in the 3rd order polynomial, rational function and MMF models. It is interesting to note that as order of the basin increased, senility of the landscape increased and logistic and yield density model of Harris have been best fit. The basin 4.006 with 3rd degree polynomial fit has a hypsometric curve typical of early mature stage. However, it must be kept in mind that it is very difficult and not always desirable to estimate the cyclical stage of evolution just from the geometry of hypsometric curve and the best-fit ones.

Table – 2: Regression Parameters of Best-fit Curves

1)	**Harris Model: $y = 1 / (a+b.x^c)$**			
	Basin – 6.001	$y = 1 / (1.36453 + 12.92322\ x^{0.78004})$	$S_E = 0.20189$	$R^2 = 0.62$
	Basin – 5.001	$y = 1 / (1.28173 + 8.46026\ x^{0.92447})$	$S_E = 0.17432$	$R^2 = 0.73$
	Basin – 4.001	$y = 1 / (1.29290 + 9.57147\ x^{0.94799})$	$S_E = 0.18081$	$R^2 = 0.72$
2)	**Logistic Model: $y = a /(1+b.e^{-cx})$**			
	Basin – 5.002	$y = 0.04081 /(1 + 0.94895.\ e^{-0.81410\ x})$	$S_E = 0.16706$	$R^2 = 0.74$
3)	**3rd Degree Polynomial Fit: $y = a+bx+cx^2+dx^3$**			
	Basin – 4.006	$y = 0.97478 –2.09565x+3.60804x^2–2.46466x^3$	$S_E = 0.03$	$R^2 = 0.99$
4)	**Rational Function: $y = (a+bx) /(1+cx+dx^2)$**			
	Basin – 4.007	$y = (0.94982–0.95185x)/(1+1.41077x–1.96834x^2)$	$S_E = 0.04409$	$R^2 = 0.99$
5)	**MMF Model: $y = (a.b + c.x^d)/(b + x^d)$**			
	Basin – 4.002	$y = \{(0.96423)(–0.00000009) + 0.00000085.x^{0.52758})\} /(– 0.00000009+x^{0.52758})$	$S_E = 0.07935$	$R^2 = 0.98$
	Basin – 4.003	$y = \{(1.03856)(0.32628) – 0.28558.x^{0.65362})\} /(0.32628 + x^{0.65362})$	$S_E = 0.02248$	$R^2 = 0.99$
	Basin – 4.004	$y = \{(1.02058)(14.47206) – 14.60281.x^{0.25040})\} /(14.47206 + x^{0.25040})$	$S_E = 0.02571$	$R^2 = 0.99$
	Basin – 4.005	$y = \{(1.00741)(3179.7285) – 3053.6164.x^{0.39280})\} /(3179.7285 + x^{0.39280})$	$S_E = 0.05214$	$R^2 = 0.98$

Multiple Correlation Analysis

For multivariate analysis, a GDM of (43 × 13) dimension with 13 parameters and 43 basins of 3rd, 4th, 5th and 6th orders have been derived for varying locations, geometry, morphometry and morphology (Appendix – I). The principal descriptive statistical measures of these 13 variables have been computed from the data matrix for the hypsometric analysis of the 43 basins (Table – 3). All these are ratio data and are first explored for inter-variable statistical association.

The basin begins from an elevation of 7m and finally reaches 343m with a range of about 336 m. Besides this, other parameters with significant ranges are drainage texture, stream frequency, L/W ratio, and drainage density. Data variability is above 100% in cases of drainage texture and roughness index; it is close to 100% in case of basin slope, relief and stream frequency. Variability lies between 30 to 50% in cases of drainage density, dissection index, hypsometric integral, and between 20 – 30% in cases of L/W ratio and form factor; circularity ratio has a variability close to 20%, while the lowest variability is found in case of compactness coefficient (9.6%) followed by elongation ratio (10.2%). Naturally, variance is highest in case of basin relief; besides this the only variable with significant variance is drainage texture. All the thirteen variables have positively skewed distribution, significant one being the basin slope only. Distribution of all the variables are broadly platykurtic, except basin slope which is leptokurtic and hypsometric integral, form factor, ruggedness index, stream frequency and drainage texture which are close to mesokurtic one.

A correlation matrix (Table – 4) has been drawn to identify the kind of significant

Table – 3: Descriptive Statistics of the Basin Parameters

Parameter	Mini mum	Maxi mum	Mean	Standard Deviation	Vari-ance	Skew ness	Kurtosis
HI: Hypsometric integral	0.154	0.630	0.370	0.130	0.017	0.132	-1.058
L / W ratio	1.207	3.260	2.057	0.534	0.285	0.553	-0.164
C_R: Circularity ratio	0.364	0.847	0.549	0.104	0.011	0.385	0.082
E_R: Elongation ratio	0.473	0.793	0.624	0.064	0.004	0.024	0.740
C_C: Compactness coefficient	1.087	1.659	1.368	0.131	0.017	0.270	-0.525
F_F : Form factor	0.176	0.494	0.309	0.063	0.004	0.418	0.947
B_R : Basin relief (m)	7.000	343.00	105.802	86.620	7503.0	1.105	0.177
θ : Basin slope (degree)	0.009	0.190	0.038	0.037	0.001	2.153	5.588
DI : Dissection Index	0.163	0.940	0.498	0.176	0.031	0.228	-0.269
R_I : Ruggedness index	0.012	0.635	0.161	0.167	0.028	1.265	0.848
S_F : Stream frequency (No./ sq km)	0.139	5.893	1.563	1.301	1.693	1.136	1.241
D_d : Drainage density (km / sq km)	0.416	2.677	1.369	0.640	0.410	0.379	-1.053
D_T : Drainage texture	0.058	13.521	2.878	3.219	10.361	1.382	1.616

Source: Computed by the authors

Table – 4: Correlation Matrix of the Basin Parameters

	HI	L/W	C_R	E_R	C_C	F_F	B_R	θ	DI	R_I	S_F	D_d	D_T
HI	1												
L/W	-0.23	1											
C_R	**0.55**	-0.39	1										
E_R	0.36	**-0.81**	**0.65**	1									
C_C	**-0.56**	0.37	**-0.99**	**-0.63**	1								
F_F	0.36	**-0.80**	**0.65**	**0.99**	**-0.62**	1							
B_R	**-0.78**	0.06	**-0.70**	-0.23	**0.73**	-0.23	1						
θ	**-0.57**	0.03	**-0.53**	-0.21	**0.55**	-0.22	**0.78**	1					
DI	**-0.63**	0.31	**-0.73**	-0.42	**0.72**	-0.43	**0.84**	**0.56**	1				
R_I	**-0.72**	-0.02	**-0.60**	-0.21	**0.61**	-0.21	**0.86**	**0.70**	**0.63**	1			
S_F	-0.08	-0.29	0.00	0.11	-0.01	0.11	0.12	0.28	-0.21	0.44	1		
D_d	-0.32	-0.21	-0.16	-0.02	0.15	-0.02	0.30	0.41	-0.02	**0.65**	**0.91**	1	
D_T	-0.12	-0.24	-0.03	0.06	0.02	0.06	0.15	0.30	-0.15	0.49	**0.98**	**0.91**	1

Source: Computed by the authors

relationships between the variables. It shows that –

(a) hypsometric integral (HI) bears significantly positive correlation with {C_R} and negative relations with {C_C, B_R, θ, DI, R_I},

(b) significantly positive correlations emerge between C_R and {E_R, F_F}, E_R and {C_R, F_F}, C_C and {B_R, θ, DI, R_I}, F_F and {C_R, E_R}, B_R and {C_C, θ, DI, R_I}, θ and {C_C, B_R, DI, R_I}, DI and {C_C, B_R, θ, R_I}, R_I and {C_C, B_R, θ, DI, D_d}, S_F and {D_d, D_T}, D_d and { R_I, S_F, D_T}, and D_T and {S_F, D_d},

(c) significantly negative correlations lie between HI and {C_C, B_R, θ, DI, R_I}, L/W and {E_R, F_F}, C_R and {C_C, B_R, θ, DI, R_I}, E_R and {L/W, C_C}, C_C and {HI, C_R, E_R, F_F}, F_F and {L/W, C_C}, B_R and {HI, C_R}, θ and {HI, C_R}, DI and {HI, C_R}, and R_I and { HI, C_R}.

Factor Analysis

Different denudational rates and erosional stages may be present even within a single basin. A basin may be getting stripped of its rock and soil veneer overall but not at the same rates throughout, if it is presumed that the whole basin was subjected to the action of exogenic forces at the same time initially. Different sections of the basin may have evolved at different times, some sub-basins may have formed due to fragmentation or coalescing of other basins and as such experienced varying denudation chronology. Differing lithology too leads to sudden changes in the curve profile, as in the case of Basin 4B, wherein half the basin lies within the more resistant plateau fringe (crystalline rocks) and half over the relatively easily worn gravel beds. The junction between these two formations is sharp and effect of the steeper plateau scarps standing above the rolling gravel plain is reflected in the jerkiness of the mid-profile section.

Factor analysis has been done to extract factor scores, in order to identify the hypsometric classes. From the initial data matrix, eigen values (Table – 5) have been extracted for 13 components by principal component analysis (PCA) method using SPSS. With a view to maximizing the goodness of fit in the 13-dimensional space, varimax rotation of the principal components has been performed (Table – 6). Analysis has been done considering an initial communality of 1.0 for all the thirteen variables. After the extraction of eigen values, communality reduced, highest being 0.971 (stream frequency) and the lowest 0.654 (hypsometric integral). Three principal components with eigen values above 1.0 have been extracted as significant ones. These together explain 87.24% of the variation in the (43 × 13) data matrix.

Initially the first component accounted for 46.12%, second component 27.40% and the third component 13.72% of the total variation. After varimax rotation, the goodness of fit increased in the scatter plots in the 13 – dimensional space and the proportion of the components finally adjusted as follows— 1st component (37.51%), 2nd component

Table 5: Extraction of Eigen Values by Principal Component Analysis

Parameters	Communality		Compo-nent	Initial Eigen Values			Eigen Values after Varimax Rotation		
	Initial	Extracted		Total	Variance (%)	Cumulative (%)	Total	Variance (%)	Cumulative (%)
HI	1	0.654	1	5.9955	46.12	46.12	4.88	37.51	37.51
L/W	1	0.811	2	3.5620	27.40	73.52	3.26	25.06	62.57
C_R	1	0.830	3	1.7841	13.72	87.24	3.21	24.68	87.24
E_R	1	0.970	4	0.5909	4.55	91.79			
C_C	1	0.824	5	0.3986	3.07	94.86			
F_F	1	0.963	6	0.2725	2.10	96.95			
B_R	1	0.966	7	0.1733	1.33	98.29			
θ	1	0.679	8	0.1129	0.87	99.15			
DI	1	0.853	9	0.0576	0.44	99.60			
R_I	1	0.907	10	0.0311	0.24	99.84			
S_F	1	0.971	11	0.0131	0.10	99.94			
D_d	1	0.949	12	0.0066	0.05	99.99			
D_T	1	0.965	13	0.0012	0.01	100.00			

Source: Computed by the authors

Table – 6: Component Score (Factor Loading) Matrix

Parameter	Unrotated Component Scores			Parameter	Rotated Component Scores		
	1	2	3		1	2	3
C_R	-0.888	0.203	0.006	B_R	0.979	-0.018	0.084
C_C	0.887	-0.189	0.032	DI	0.860	-0.245	-0.231
B_R	0.862	0.159	0.444	R_I	0.834	-0.025	0.459
R_I	0.818	0.455	0.175	HI	-0.779	0.185	-0.114
DI	0.805	-0.239	0.385	θ	0.777	-0.023	0.273
HI	-0.777	-0.075	-0.211	C_C	0.755	-0.504	0.005
θ	0.731	0.295	0.242	C_R	-0.735	0.538	-0.013
F_F	-0.648	0.492	0.548	E_R	-0.220	0.960	0.008
E_R	-0.645	0.498	0.552	F_F	-0.225	0.955	0.003
S_F	0.169	0.880	-0.410	L/W	0.031	-0.877	-0.201
D_T	0.221	0.860	-0.420	S_F	0.024	0.105	0.980
D_d	0.380	0.833	-0.333	D_T	0.061	0.063	0.978
L/W	0.405	-0.635	-0.493	D_d	0.238	0.033	0.944

Source: Computed by the authors

(25.06%), and 3rd component (24.68%). Initially, the contributions of the 1st component has been better explained by the variations in the values of circularity ratio, compactness coefficient, basin relief ruggedness index, dissection index and hypsometric integral and the contributions of the 2nd component by the variations in the values of stream frequency, drainage texture and drainage density. After rotation, the 1st component has been better explained by the variables of basin relief, dissection index, and ruggedness index, the 2nd component by elongation ratio, form factor and L/W ratio while the 3rd component by the stream frequency, drainage texture and drainage density. Based on the magnitudes of the principal components and the factor loadings, factor scores for each basin have been computed (Table – 7).

Basin Classes

a) *Based on Factor Plots*

The scatter plots of Factor – 1 and Factor – 2 can be ideally used to identify hypsometric classes of basins and sub-basins. Clusters of lineations may be identified in the scatter of points, each of which represents a distinctive hypsometric class (Table – 8, Fig. 7).

In four quarters of the graph, altogether nine lineations and 3 outliers representing twelve hypsometric classes of basins and sub-basins have been identified— two in the north east, four in the north west, three in the south west and three in the south east quarters. Thus, class – I contains one 5th, one 4th and one 3rd order sub-basins, class – II one 5th, one 4th and two 3rd order sub-basins, class – III four 3rd order sub-basins, class – IV one 4th and six 3rd order sub-basins, class – V two 3rd order sub-basins, class – VI and Class – VII two 4th order and four 3rd order sub-basins each, class – VIII five 3rd order sub-basins, class – IX one 4th and two 3rd order sub-basins, and three outliers comprising the main Dulung basin (6.001) and two 3rd order sub-basins, viz., 3.018 and 3.023. Thus, from the scatter plots of factor scores, twelve distinctive classes of basins and sub-basins have been identified (Table – 8).

b) *Based on Factor Score*

The hypsometric quality of a basin depends on its surface geology, network parameters, geometric parameters, morphological and finally morphometric parameters. Scores on the first factor can be ideally used for the purpose of classifying the basins and sub-basins based on the properties of the 13 parameters of the 43 Dulung N basin and its sub-basins. Factor score varies from a minimum of -1.515 to 2.590 within the

Table – 7: Factor Score Matrix

Basin ID	Factor – 1	Factor – 2	Factor – 3	Basin ID	Factor – 1	Factor – 2	Factor – 3
6.001	2.590	-0.128	-1.020	3.023	-0.367	-2.499	-0.637
5.002	1.988	1.905	-0.348	3.016	-0.408	-1.204	-0.868
4.003	1.814	0.609	1.110	4.006	-0.423	-1.012	-0.526
5.001	1.604	0.260	-0.961	3.014	-0.428	0.958	-0.453
4.001	1.532	1.216	-1.017	3.025	-0.474	0.277	-0.393
3.002	1.492	0.932	-0.037	3.015	-0.482	-0.081	0.428
3.007	1.273	-0.644	1.960	3.026	-0.532	1.132	-0.452
4.004	1.077	-0.348	1.007	3.029	-0.593	-1.320	-1.106
3.012	0.990	0.094	0.650	3.021	-0.597	1.011	-0.653
3.001	0.929	0.215	0.026	3.027	-0.620	0.146	-0.957
3.013	0.897	-2.233	-0.095	3.022	-0.690	0.131	0.883
3.011	0.531	-1.302	1.226	3.017	-0.739	0.083	-0.764
3.008	0.400	-0.696	1.148	3.019	-0.777	0.874	-0.687
3.009	0.358	-0.067	1.626	4.002	-0.785	-0.361	0.575
3.004	0.123	-0.414	0.388	3.020	-0.821	0.432	-0.563
3.010	0.029	-0.127	1.696	3.005	-0.903	0.745	0.731
4.007	-0.206	-0.900	-0.626	3.018	-0.938	2.586	-0.884
3.032	-0.231	-0.733	-1.226	3.024	-1.000	-0.413	-0.634
3.028	-0.276	0.744	-0.981	3.031	-1.361	0.836	1.164
4.005	-0.325	-0.307	-0.943	3.006	-1.457	1.173	2.709
3.033	-0.335	-0.093	-1.002	3.030	-1.515	-0.471	1.074
3.003	-0.341	-1.007	-0.563				

Source: Computed by the author

Table – 8: Basin Classes based on Factor Plots

Quadrant	Lineation / Class	Basins/ Sub-basins Cluster
1. NE	I	{5.002, 4.001, 3.002}
	II	{5.001, 4.003, 3.012, 3.001}
2. NW	III	{3.028, 3.026, 3.021, 3.014}
	IV	{4.002, 3.02, 3.027, 3.025, 3.022, 3.017, 3.005}
	V	{3.031, 3.006}
	VI	{3.018}
3. SW	VI	{4.005, 4.002, 3.033, 3.030, 3.024, 3.015}
	VII	{4.007, 4.006, 3.032, 3.029, 3.016, 3.003}
4. SE	VIII	{3.013, 3.011, 3.010, 3.008, 3.004}
	IX	{4.004, 3.009, 3.007}
Outliers	X	{6.001}
	XI	{3.023}
	XII	{3.018}

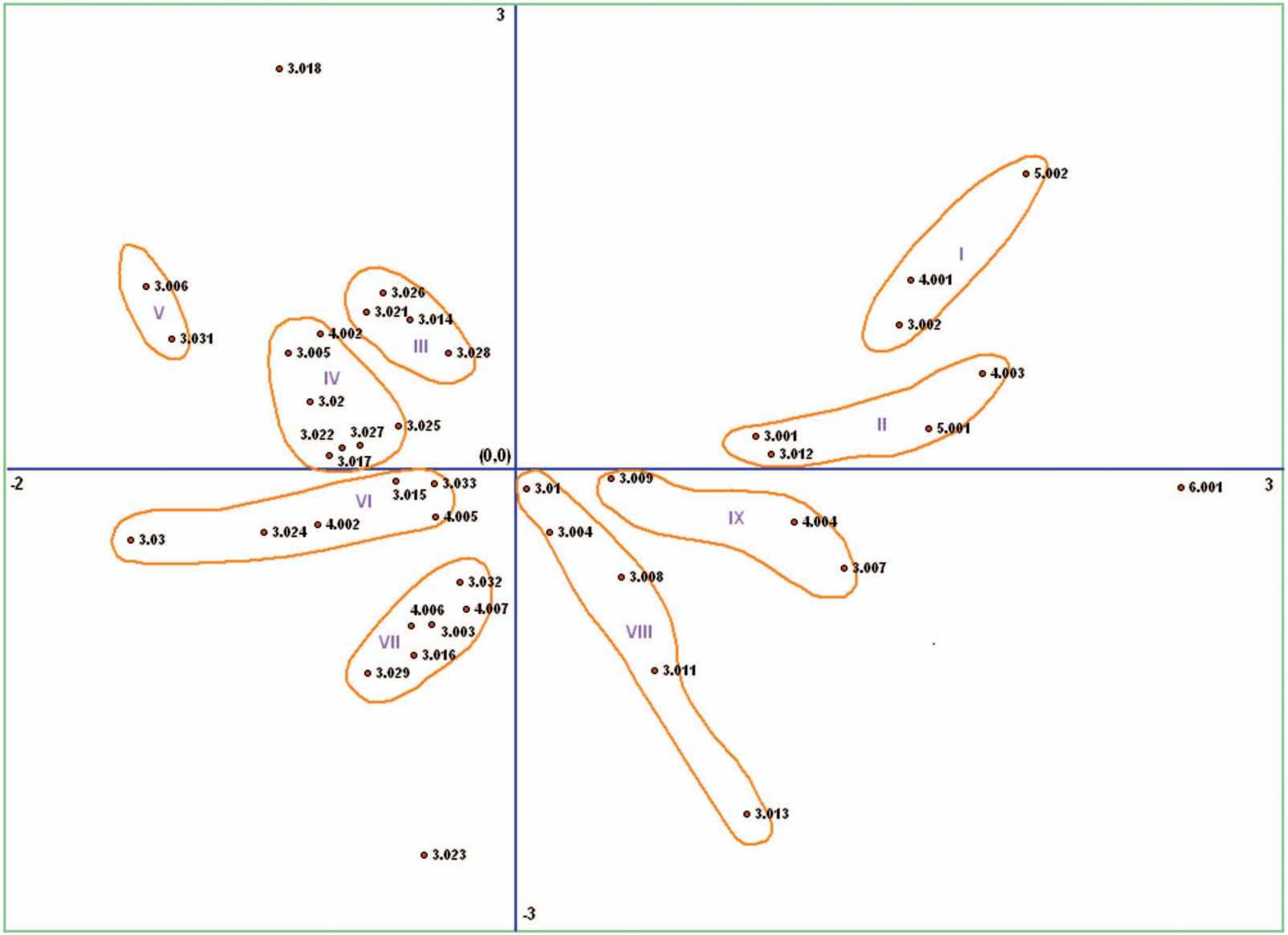

Fig. 7: Scatter Plots showing Clusters

43 basins and sub-basins. A five class distribution has been done with two open end classes, as follows—

Factor Score 1	Basins & Sub-basins
1. ≥ 2	:{6.001}
2. 1 – 2	:{5.002, 4.003, 5.001, 4.001, 3.002, 3.007, 4.004}
3. 0 – 1	:{3.012, 3.001, 3.013, 3.011, 3.008, 3.009, 3.004, 3.010}
4. – 1 to 0	:{4.007, 3.032, 3.028, 4.005, 3.033, 3.003, 3.023, 3.016, 4.006, 3.014, 3.025, 3.015, 3.026, 3.029, 3.021, 3.027, 3.022, 3.017, 3.019, 4.002, 3.020, 3.005, 3.018}
5. ≤ – 1	:{3.024, 3.031, 3.006, 3.030}

Thus, based on factor scores, five distinctive classes have been identified. Class 1 contains the main basin, class 2 seven sub-basins (5^{th} order = 2, 4^{th} order =3, 3^{rd} order =2), class 3 eight 3^{rd} order sub-basins, class 4 twenty three sub-basins (4^{th} order = 4, 3^{rd} order = 19), and class 5 four 3^{rd} order sub-basins.

Conclusion

Thus, hypsometric curves vary in shapes and hypsometric integrals. The nature of correlations also varies as extrinsic controls are many and vary in magnitudes and sense. Hence, the intrinsic control of the underlying geology and the denudation chronology must be taken into account for explaining the significant variations with further elaborations. However, hypsometric curves are not an absolute indicator of the basin evolutionary processes or present condition. At best they are an "at-that-moment volumetric evaluation" of the likely geomorphic status of an otherwise constantly changing land surface. Even demarcating terrain units based on the hypsometric integrals can prove hazardous and oversimplified since it is an indicator only. Furthermore, the shape of the basin can significantly influence area-height distribution within a catchment, especially in leaf-shaped dendritic basins, wherein both the basin head and mouth regions may be narrow (in which case the basin relief value assumes much importance in determining the hypsometric integral and especially in case of Basin 4.006, a narrow mouth is reflected in the curve as a sharp drop that further accentuates the curve's convexity), or in basins arising on relatively level, rolling plateau tops and descending onto a primarily flat and low plain with the steeper plateau-edge scarps sandwiched in between (smaller 'a' values betwixt larger 'a' values giving rise to curves that may fluctuate more than once, even across the equilibrium line) or in structurally controlled narrow basins.

Bibliography

1. Chorley, R J (1957): Illustrating the Laws of Morphometry, *Geol. Mag.,* 94(2), pp140 – 150.
2. Davis, W M (1899): The Geographical Cycle, *Geographical Journal*, Vol.14, pp 481–504.
3. Evans, I S (1979): Hypsometry, statistics, and simplicity – a comment. *Intl. Jour. Assoc. Math. Geol.* 11(1).
4. Harlin, J M (1979): Reply to hypsometry, statistics, and simplicity: In defense of a second function. *Intl. Jour. Assoc. Math. Geol.* 11(1).
5. Horton, R E (1932): Drainage basin characteristics, *Trans. Am. Geophys. Union,*13, pp350 – 361.
6. Horton, R E (1945): Erosional development of streams and their drainage basins – hydrophysical approach to quantitative morphology, *Geol. Soc. Amer. Bull.,* 56, pp275 – 370.
7. Huang, X (2007): How do streamflow generation mechanisms affect watershed hypsometry? *Earth Surface Processes and Landforms,*132(2).
8. Langbein, W B, and Basin, W (1947): Topographic characteristics of drainage basins, USGS *Water-Supply Paper*: 947-C.
9. Langbein, W B, et al (1947): Topographic characteristics of drainage basins. USGS *Water-Supply Paper*: 968-C: 125 –158.
10. Luo, W (2003): A theoretical travel time based on watershed hypsometry, *Jour. Amer. Wat. Resour. Assoc.,* 39(4).
11. Nag, S K (1998): Morphometric analysis using remote sensing techniques in the Chaka sub-basin, Purulia District, West Bengal, *Jour. Ind. Soc. Remote Sensing*, 26(1&2), pp69 – 76.
12. Patel, P P and Sarkar A (2008): Hypsometric analysis of the Dulung N. basin and its sub-

Appendix I: GDM for Basin Parameters

B_ID	HI	L/W	C_R	E_R	C_C	F_F	B_R	θ	DI	R_I	S_F	D_d	D_T
3.031	0.630	1.500	0.698	0.694	1.197	0.378	12	0.021	0.273	0.025	3.062	2.061	6.310
3.006	0.592	1.332	0.674	0.735	1.218	0.424	23	0.023	0.181	0.053	5.893	2.294	13.521
3.030	0.573	1.840	0.609	0.605	1.281	0.287	7	0.022	0.163	0.011	3.103	1.639	5.084
3.032	0.565	2.342	0.495	0.581	1.422	0.265	71	0.015	0.724	0.031	0.181	0.430	0.078
3.026	0.559	1.379	0.589	0.703	1.303	0.389	44	0.018	0.358	0.052	0.952	1.192	1.134
4.006	0.513	2.374	0.481	0.567	1.441	0.253	70	0.015	0.530	0.073	0.752	1.048	0.787
3.025	0.513	1.671	0.537	0.647	1.365	0.329	52	0.018	0.397	0.060	1.026	1.147	1.177
3.027	0.495	2.046	0.616	0.637	1.274	0.319	49	0.012	0.480	0.032	0.245	0.660	0.162
3.029	0.491	3.063	0.540	0.561	1.361	0.247	63	0.013	0.618	0.026	0.139	0.416	0.058
3.033	0.482	2.142	0.599	0.616	1.292	0.298	59	0.014	0.694	0.043	0.424	0.720	0.305
3.014	0.480	1.657	0.563	0.705	1.333	0.390	49	0.016	0.340	0.058	0.976	1.189	1.161
3.018	0.479	1.328	0.847	0.793	1.087	0.494	24	0.009	0.231	0.015	0.679	0.646	0.438
3.021	0.475	1.775	0.676	0.695	1.217	0.379	54	0.016	0.409	0.054	0.723	0.998	0.722
3.005	0.463	1.592	0.644	0.685	1.246	0.368	36	0.024	0.257	0.061	2.728	1.694	4.623
4.007	0.418	2.976	0.470	0.611	1.459	0.293	74	0.017	0.565	0.079	0.781	1.063	0.831
3.020	0.417	1.946	0.675	0.656	1.217	0.338	35	0.011	0.350	0.034	0.680	0.975	0.663
3.019	0.416	1.635	0.715	0.672	1.182	0.355	36	0.013	0.346	0.032	0.496	0.897	0.445
3.024	0.404	2.500	0.650	0.612	1.240	0.294	29	0.010	0.333	0.023	0.507	0.782	0.397
4.002	0.398	2.405	0.572	0.632	1.322	0.314	46	0.025	0.324	0.075	2.424	1.621	3.929
3.017	0.389	1.907	0.638	0.623	1.252	0.305	43	0.011	0.350	0.027	0.514	0.628	0.323
3.016	0.375	2.408	0.465	0.552	1.467	0.239	56	0.015	0.418	0.032	0.225	0.580	0.130
3.022	0.374	1.663	0.608	0.633	1.283	0.315	43	0.024	0.355	0.085	2.569	1.979	5.085
3.028	0.370	1.684	0.620	0.668	1.270	0.351	47	0.015	0.511	0.035	0.338	0.745	0.252
3.008	0.349	2.080	0.460	0.570	1.474	0.255	143	0.075	0.528	0.293	3.028	2.049	6.205
3.023	0.346	3.260	0.429	0.473	1.527	0.176	74	0.015	0.565	0.062	0.485	0.841	0.408
4.005	0.340	2.210	0.532	0.614	1.371	0.296	59	0.013	0.440	0.035	0.318	0.595	0.189
3.002	0.325	1.207	0.386	0.664	1.609	0.347	174	0.116	0.542	0.273	1.657	1.569	2.599
3.007	0.302	2.580	0.437	0.581	1.513	0.265	237	0.103	0.649	0.635	3.636	2.677	9.736
3.015	0.281	2.081	0.653	0.614	1.238	0.297	71	0.026	0.438	0.123	1.956	1.747	3.418
3.003	0.279	2.957	0.542	0.583	1.358	0.267	83	0.017	0.459	0.092	0.482	1.107	0.534
3.011	0.269	2.065	0.412	0.517	1.557	0.210	135	0.071	0.538	0.313	2.619	2.320	6.075
3.012	0.255	1.896	0.521	0.599	1.385	0.282	194	0.091	0.626	0.382	2.287	1.969	4.502
3.001	0.246	2.257	0.528	0.626	1.376	0.308	187	0.105	0.560	0.282	1.638	1.505	2.466
3.004	0.236	2.358	0.567	0.594	1.328	0.277	115	0.052	0.523	0.210	1.814	1.823	3.306
4.003	0.236	1.416	0.411	0.633	1.560	0.315	261	0.067	0.715	0.594	3.080	2.277	7.015
5.001	0.235	1.825	0.403	0.619	1.574	0.301	261	0.043	0.781	0.252	0.747	0.967	0.723
3.010	0.220	2.178	0.591	0.621	1.301	0.303	113	0.049	0.507	0.289	3.400	2.560	8.704
4.001	0.206	1.688	0.469	0.689	1.460	0.373	238	0.051	0.713	0.238	0.662	0.999	0.661
4.004	0.205	2.208	0.479	0.585	1.444	0.269	207	0.064	0.666	0.474	2.561	2.292	5.869
6.001	0.188	2.587	0.416	0.572	1.550	0.257	343	0.190	0.940	0.302	0.597	0.881	0.526
5.002	0.187	1.237	0.492	0.715	1.425	0.401	292	0.036	0.800	0.467	1.601	1.600	2.561
3.009	0.177	1.945	0.535	0.617	1.367	0.299	133	0.054	0.530	0.302	3.829	2.272	8.698
3.013	0.154	3.260	0.364	0.482	1.659	0.182	208	0.037	0.671	0.293	1.391	1.407	1.958

Source: Values acquired and compiled by the authors

basins, *Geographical Review of India*, 36 (4), pp 409 – 422.
13. Pike, R J and Wilson, S E (1971) : Elevation-Relief Ratio, Hypsometric Integral, and Geomorphic Area-Altitude Analysis, *GSA Bulletin,* 82 (4), pp1079-1084.
14. Rao, J U, et al (1995): A quantitative morphometric analysis of Gundalakamma river basin, Andhra Pradesh, *Ind. Jour. Earth Science*, 22(1 & 2), pp 63 – 74.
15. Sarkar, A (1994): 2nd Order TDCN Configuration – an alternative approach, *Ind. Jour. Earth Science*, 21(4), pp 226 – 235.
16. Sarkar, A (1995): Morphometric identity of TDCN basins – a case study of Lodham Khola basin, Darjeeling Himalayas, *Ind. Jour. Geol.*, 67(2), pp 142 – 150.
17. Sarkar, A (1997): Identification of the 2nd Order TDCN basin properties of Lodham Khola in Darjeeling Himalayas, *Ind. Jour. Earth Science*, 24(1 & 2), pp 47 – 54.
18. Sarkar, A (2007): Statistical analysis of drainage networks – a study in the BMB - CGC Complex, *Ind. Jour. Landscape System and Ecological Studies*, 30(1), pp 5 –16.
19. Strahler, A N (1952): Hypsometric analysis of erosional topography, *Geol. Soc. Amer. Bull.,* Vol. 63, pp1117 – 1142.
20. Strahler, A.N (1957): Quantitative analysis of watershed geomorphology, *Trans. Amer. Geophys. Union*, Vol. 38, pp 913 – 920.

Prof Ashis Sarkar

Head, Department of Geography, Presidency University, Kolkata – 700 073

Priyank Pravin Patel

Assistant Professor, Department of Geography, Aliah University, Kolkata – 700 091